Inertial particle collisions in turbulent synthetic flows: Quantifying the sling effect

Lauris Ducasse[1] and Alain Pumir[2]
[1]*Institut Non Linéaire de Nice, CNRS, F-06560 Valbonne, France*
[2]*Laboratoire de Physique, Ecole Normale Supérieure de Lyon, 46 Allée d'Italie, F-69007 Lyon, France*
(Received 21 August 2009; published 16 December 2009)

Turbulent motion increases very significantly the collision rate between particles in dilute suspensions. In the case of heavy inertial particles, the collision rate enhancement results both from the intermittent concentration in the flow, and also from the large relative velocity between colliding particles. The latter effect is a consequence of the ejection of particles out of curved streamlines, denoted here as the "sling effect." Here, we quantitatively study the collision rate between heavy particles in the presence of gravity, with the simplified synthetic model of turbulent flow known as kinematic simulation. Monitoring the velocity of colliding particles and comparing it with the local velocity gradient of the flow of particles allowed us to identify the collision induced by the sling effect and to evaluate their contribution to the total collision rate. Our numerical results are then systematically compared with the estimates based on the properties of particle trajectories in the flow recently proposed by Falkovich and Pumir [G. Falkovich and A. Pumir, J. Atmos. Sci. **64**, 4497 (2007)]. At moderate values of the Stokes numbers ($\mathrm{St} \lesssim 1$), we demonstrate that the resulting parametrization describes quantitatively correctly the collision rate, and that the sling effect can be responsible for up to $\sim 50\%$ of the total collision rate.

DOI: 10.1103/PhysRevE.80.066312 PACS number(s): 47.55.df, 45.50.−j, 92.60.Mt, 42.68.Bz

I. INTRODUCTION

Turbulent fluid motion notoriously plays a strong role in enhancing the collision rate between particles [1] and, in turn, the rate of coalescence in a variety of natural and engineering situations. This phenomenon has been identified to be important, among others, for the transport of dust and pollutants in air, of sediments in rivers, and for the growth of liquid vapor droplets in warm clouds, ultimately leading to the formation of raindrops [2]. The present work is motivated to a large extent by the latter effect. In warm clouds, tiny droplets of size ~ 1 μm are nucleated by aerosols. Collisions induced by turbulence are expected to be particularly important for determining the rate of coalescence of droplets of size $\sim 10-20$ μm, at a stage where the droplet size distribution is quite narrow. In clouds, the size of the droplets is much smaller than the Kolmogorov length, i.e., the smallest length scale of turbulence: $\eta \sim 1-10$ mm.

The aim of this work is to study the enhancement of the collision rate of a system of heavy particles of small size a ($a \ll \eta$) by turbulence. In general, the collision rate per unit of volume $K(a)$ between particles of equal size, of diameter a, and of mean density n_0 can be written as [3,4]

$$K(a) = \pi n_0^2 a^2 \langle |w_r| \rangle g(a), \tag{1}$$

where $w_r = \mathbf{w} \cdot \hat{r}$ is the radial relative velocity between two particles and $g(a)$ is the radial distribution function at contact.

Particles with negligible inertia and in the absence of gravity exactly follow the fluid and remain uniformly distributed, so that $g(a)=1$. In this case, the collision rate is enhanced by the strong velocity gradients in the flow. The resulting expression for the collision rate has been derived in the seminal work of Saffman and Turner [1],

$$K_{ST} = \frac{1}{2} n_0^2 a^3 \left(\frac{8\pi}{15} \right)^{1/2} \frac{1}{\tau_K}, \tag{2}$$

where τ_K is the Kolmogorov time. The collision rate can also be estimated analytically in the case of particles with so much inertia that they do not really follow the turbulent flow, but rather move with a random essentially Gaussian turbulent velocity. In this case, the collision rate can be estimated from gas kinetic theory [5],

$$K_{KT} = \frac{1}{2} n_0^2 a^2 \left(\frac{6\pi}{3} \right)^{1/2} \langle v^2 \rangle^{1/2}, \tag{3}$$

where $\mathbf{v}$ is the velocity of the particles. In the two cases above, the collision rate is completely determined by a single quantity characterizing the flow, the Kolmogorov time [Eq. (2)] or the kinetic energy of the particles [Eq. (3)].

Such a simple parametrization does not exist in the general case of particles with finite inertia. The enhancement of the collision rate, observed in many direct numerical studies (DNSs), can be potentially attributed to either of the two terms on the right-hand side of Eq. (1): $g(a)$ or $\langle |w_r| \rangle$. The preferential concentration phenomenon, whereby inertial particles distribute very inhomogeneously in the flow, effectively leads to clustering of particles, and hence to values of $g(a)$ larger than 1. The enhancement of the relative velocity, $\langle |w_r| \rangle$, comes from inertial effects. The effective velocity gradient tensor of the particle velocity field can be significantly stronger than the underlying velocity gradient of the fluid. In particular, because particles do not follow exactly the fluid, particles originating from different regions in the flow may catch up with one another, thus leading to an infinitely large particle velocity gradient. This effect, introduced and named in [6], can be explained in terms of the formation of caustics of particle trajectories [7] in the flow. It raises the possibility

of collision of jets of particles with velocity difference of order $\langle u^2\rangle^{1/2}$, thus leading to a significant increase in the relative velocity $\langle w_r\rangle$.

In a recent attempt to quantify the importance of the two effects, Falkovich and Pumir [8] proposed to decompose the collision rate as a sum of two contributions. The "continuous" contribution accounts for the collisions between particles whose velocity difference can be described quantitatively by the (smooth) gradient of the particle velocities, and a "sling" contribution, due to the collisions between particles originating from very different regions of the flow, with a velocity difference of order 1. This decomposition can be formulated in terms of properties of Lagrangian trajectories of particles in the flow, thus leading to the indirect Lagrangian method (ILM), originally proposed in [8]. Indeed, the predictions of this approach seem to agree reasonably well with results obtained by directly counting the number of collisions in a flow, at least under conditions where the contribution of the caustics is weak compared to the continuous term [8]. The Lagrangian approach certainly captures the enhancement of the collision rate observed in DNS. Whether the parametrization proposed in [8] correctly captures the enhancement due to the sling term has however not been properly demonstrated.

It should be stressed that the sling effect is intrinsically difficult to describe because it corresponds to a failure of any hydrodynamic description of the motion of particles, induced by the multivalued nature of the particle velocity field. A proper parametrization of the various effects responsible for the collision rate, a problem both of fundamental importance and potentially very significant for a number of applications, is the main objective of this work. To this end, we carried out a direct comparison between the proposed way of parametrizing the collision rate [8] and simulations directly counting the total number of collisions. One of the major difficulties of this approach is that the time needed to simulate a Navier-Stokes flow at a reasonable Reynolds number in the presence of many particles can be prohibitively large. In addition, in its simplest form, the problem of determining the collision rate of inertial particles in a turbulent flow, in the presence of gravity, involves three dimensionless numbers. The Reynolds number Re parametrizes the intensity of turbulence or, equivalently, the ratio of scales in the flow $\mathrm{Re}=(L/\eta)^{4/3}$, where $L(\eta)$ is the integral (Kolmogorov) scale. The Stokes number St defines the ratio between the response time of the particles, τ_P, and the Kolmogorov time scale $\tau_K=\eta^2/\nu$ (where ν is the fluid viscosity) characterizing the smallest structures of the flow. The Stokes number is simply related to the ratio between the diameter a of the particle and the Kolmogorov length by the relation $\eta/a=\Psi\,\mathrm{St}^{-1/2}$, with $\Psi=[\frac{1}{18}(\rho_P/\rho_f)]^{1/2}$, where ρ_P (ρ_f) is the density of the particles (fluid). We will assume here that the ratio $\rho_P/\rho_f=1000$ ($\Psi\approx 7.5$), corresponding to water droplets in air. Lastly, the Froude number $\mathrm{Fr}=u_K/g\tau_P$ compares the Kolmogorov velocity, $u_K=\eta/\tau_K$, and the velocity of sedimentation $g\tau_P$. The problem is therefore characterized by three dimensionless parameters. A direct calculation of collisions in a realistic Navier-Stokes flow, with a systematic variation of the three parameters, would be prohibitively expensive. For this reason, we have chosen to carry out numerical simulations of particles using a simplified flow model, namely, the kinematic simulation (KS). Although this method has been shown to miss certain aspects of the problem of particle dispersions, it still captures several important features; it has the advantage of simplicity and leads to an easy and efficient numerical implementation. KS thus provides a very good tool to test our understanding of transport in turbulent flows. We restrict ourselves to "ghost particles," corresponding to an idealized system where colliding particles pass through each other. This approach is very often used in calculations of droplet coalescence [4,9]. The ghost particle approximation describes only the short time evolution of the system [10,11].

The paper is organized as follows. The problem of collision in a simple KS flow is formulated in Sec. II. We present the ILM of [8] in Sec. III, its numerical implementation, as well as some limitations of the method. In Sec. IV, we discuss the results from the direct calculations of the collision rates. We also explain how to separate the collisions from "sling events" from collisions originating from pairs of particles moving close to each other, thus allowing us to measure separately the continuous and the sling contributions to the collision rate. This is one of the main results of this work, which leads to very precise tests of the ILM. Section V is devoted to the comparison between the direct method and the ILM. One of the main achievements of this work is to check that the parametrization of the sling contribution is correctly captured with the help of the ideas originally proposed in [8], at least in the case of moderate Stokes numbers $\mathrm{St}\lesssim 1$. Lastly, our conclusions are presented in Sec. VI.

II. NUMERICAL SETUP OF THE PROBLEM

A. Kinematic simulations

In order to be able to carry out very long simulations at a reasonable numerical cost, we chose to describe the flow as the superposition of a finite number of random Fourier modes, rather than solving the full Navier-Stokes equations. This synthetic method, known as "kinematic simulations" [12], has been used in many dispersion problems and allows one to generate a highly turbulent flow at a very low numerical cost [13–16]. In this formulation the velocity field of the fluid is written as

$$\mathbf{u}(\mathbf{x},t)=\sum_{n=1}^{N_k}\mathbf{A}_n\cos(\mathbf{k}_n\cdot\mathbf{x}+\omega_n t)+\mathbf{B}_n\sin(\mathbf{k}_n\cdot\mathbf{x}+\omega_n t), \tag{4}$$

where N_k is the total number of Fourier modes. The orientation $\hat{\mathbf{k}}_n$ of the wave vectors $\mathbf{k}_n=k_n\hat{\mathbf{k}}_n$ are randomly chosen. The wave numbers are distributed between the large (integral) scale L and the small (Kolmogorov) scale η as

$$k_n=k_1\left(\frac{L}{\eta}\right)^{(n-1)/(N_k-1)}. \tag{5}$$

The lowest and highest wave numbers in the spectrum are chosen as

$$k_1 = \frac{2\pi}{L}, \quad k_{N_k} = \frac{2\pi}{\eta}. \tag{6}$$

The modes are uncorrelated: the orientations and the amplitudes $\mathbf{A}_n$ and $\mathbf{B}_n$ are chosen at random, perpendicular to the wave vector $\mathbf{k}_n$ to ensure incompressibility,

$$\mathbf{A}_n \cdot \mathbf{k}_n = \mathbf{B}_n \cdot \mathbf{k}_n = 0. \tag{7}$$

The norms of A_n and B_n are chosen according to

$$A_n^2 = B_n^2 = E(k_n)\Delta k_n, \tag{8}$$

where

$$\Delta k_n = \begin{cases} (k_2 - k_1)/2, & n = 1 \\ (k_{n+1} - k_{n-1})/2, & n \in [2, N_k - 1] \\ (k_{N_k} - k_{N_k - 1})/2, & n = N_k, \end{cases} \tag{9}$$

and $E(k_n)$ represents the energy spectrum, which we choose here to have the classical Kolmogorov form: $E(k_n) = E_0 k_n^{-5/3}$. In all our simulations, we took $E_0 = 1$.

We worked in a cubic numerical box $(2\pi)^3$, so the components of the $\mathbf{k}_n$ vectors must be chosen as integer values in order to fix periodic boundary conditions for the velocity field $\mathbf{u}$. To implement the periodic boundary conditions, the vectors $\mathbf{k}_n$ were determined by first specifying a vector with a random direction, and a norm given by Eq. (5), and then by finding the closest vector with integer coordinates.

Finally, the frequencies ω_n in Eq. (4) are taken to be proportional to the eddy turnover time of the mode n,

$$\omega_n = \lambda \sqrt{k_n^3 E(k_n)}, \tag{10}$$

where λ is a dimensionless parameter often referred to as the "persistence" parameter. The higher λ the faster the velocity field decorrelates. A realistic value of λ is *a priori* of order 1. It has been noticed in previous studies [13,14] that this parameter quantitatively affects the results. Our simulations have been performed for two values of λ: $\lambda = 0.5$ and 2.0, for a fixed value of the scale ratio $L/\eta = 64$ with eight modes in each band of wave numbers $[k, 2k]$.

B. Particle dynamics

Droplets before the initiation of the coalescence process are known to be much smaller than the Kolmogorov scale: typically, $\eta/a \gtrsim 100$. For particles of such a small size, and for a very dilute system, it is appropriate to use the Maxey-Riley system of equations [17]. The evolutions of the position, $\mathbf{x}(t)$, and of the velocity, $\mathbf{v}(t)$, of a particle (droplet) are described by the following differential equations:

$$\frac{d\mathbf{x}}{dt} = \mathbf{v}, \tag{11}$$

$$\frac{d\mathbf{v}}{dt} = \frac{\mathbf{u}(\mathbf{x}) - \mathbf{v}}{\tau_P} + \mathbf{g}. \tag{12}$$

In this description, an inertial particle is characterized by its dynamical time τ_P. The Stokes number is the relevant dimensionless parameter comparing the particle inertia with the Kolmogorov time: $\mathrm{St} = \tau_P/\tau_K$. The diameter a of the particle and the Stokes number are related by $\eta/a = \Psi\, \mathrm{St}^{-1/2}$ ($\Psi \simeq 7.45$ for water droplets in the air).

Due to the periodic boundary conditions in the system, particles exiting the system through one face of the periodicity box are automatically reinjected in the system through the opposite face. This does not cause any serious problem, except in the presence of a strong gravity, when the time a particle needs to settle down the system becomes comparable to or smaller than the eddy turnover time.

The equation of evolution in the Lagrangian frame of the gradient tensor $\boldsymbol{\sigma}$ of the particle velocity $\mathbf{v}(\sigma_{ij} \equiv \partial_j v_i)$ can be readily deduced from Eq. (12),

$$\frac{d\sigma_{ij}}{dt} = \frac{h_{ij} - \sigma_{ij}}{\tau_P} - \sigma_{ik}\sigma_{kj}, \tag{13}$$

where h_{ij} is the velocity derivative tensor corresponding to the fluid velocity $\mathbf{u}$ at the point of the particle: $h_{ij} = \partial_j u_i$. The nonlinear term in Eq. (13) controls the dynamics when $|\boldsymbol{\sigma}| > 1/\tau_P$, potentially leading to a divergence in a finite time for $|\boldsymbol{\sigma}|$. Physically, this could happen when a particle encounters a very strong gradient (for example, a strong vortex), so that the source term in Eq. (13) becomes large enough ($|\boldsymbol{h}| \gtrsim 1/\tau_P$) during a time of order τ_P, thus making the nonlinear term in Eq. (13) prevail.

III. ILM

A. Formulation

We use here the Lagrangian method proposed in [8] to estimate the collision rate and compare it with direct measurements. The continuous and sling contributions to the collision frequencies are estimated separately as follows. The continuous contribution is directly evaluated from a Lagrangian measurement of the gradient velocity tensor,

$$K_{cont} = \frac{n_0 a^3}{2} \left\langle \frac{1}{T} \int_0^T n(t) \int_{\hat{\mathbf{r}}\cdot\boldsymbol{\sigma}\cdot\hat{\mathbf{r}}<0} (\hat{\mathbf{r}} \cdot \boldsymbol{\sigma} \cdot \hat{\mathbf{r}}) d\Omega dt \right\rangle, \tag{14}$$

where $n_0 = N_p/V$ is the mean particle concentration in the total volume V. This approach is similar to the Saffman-Turner (ST) one. The angular brackets denote an average over many trajectories. The upper limit of the integral in Eq. (14) T corresponds to the time needed for the contraction rate along a trajectory to grow by a factor (η/a). The value of $n(t)$ is computed by integrating the continuity equation,

$$\frac{dn}{dt} = -n\sigma_{ii}. \tag{15}$$

Equations (14) and (15) can be justified by using the fact that the concentration averaged ("coarse grained") around the center of a given particle has built up from an earlier instant of time, where it was smooth at a scale $\sim\eta$. The generation of small scales results from the compression along the directions, corresponding to negative eigenvalues of the symmetric part of $\boldsymbol{\sigma}$. In practice, we follow the evolution of the inverse deformation tensor $\mathbf{W}$, which describes how a line element is transported by the flow: $\delta\mathbf{l}(t) = \mathbf{W}(t) \cdot \delta\mathbf{l}(0)$. More

precisely, we keep track of $\mathbf{W}^{-1}$ by integrating

$$\frac{d\mathbf{W}^{-1}}{dt} = -\mathbf{W}^{-1} \cdot \boldsymbol{\sigma}. \tag{16}$$

As time evolves, the norm of the matrix $|\mathbf{W}^{-1}|$ increases, which gives a quantitative measure of the small scales generated by the flow. Equation (15) indicates that concentration increases due to the compression of the velocity gradient tensor $\boldsymbol{\sigma}$. At a certain time T, the value $|\mathbf{W}^{-1}(T)|$ reached (η/a) indicating that an initially smooth concentration at scale η at $t=0$ has given rise to fluctuations down to the scale a at time T. This method has been used in [6,8] for describing the phenomenon of preferential concentration. In addition, we simply argue that the collisions affecting the particle result from the flux of particles during the time where small scales are generated, as indicated by Eq. (14) [8].

We use a phenomenological approach to estimate the sling contribution to the collision rate. A sling event is characterized by the fact that two particles can run into each other with a velocity difference of order 1, even when the separation between the two particles reaches zero. In a continuous description of the velocity field of the particles $\mathbf{v}$, this means that $\mathbf{v}$ becomes multivalued: the particle velocities have more than one value at a given point. For this reason, the evaluation of the sling contribution is intrinsically difficult. The appearance of regions in the flow where the velocity of the particles is multivalued is preceded by a singularity in a finite time for $\boldsymbol{\sigma}$ and a divergence of the concentration $n(t)$. However, because of their finite size, two particles cannot be arbitrarily close to one another, so the concentration cannot really diverge. For this reason, $|\boldsymbol{\sigma}|$ cannot grow more than a factor $\sim(\eta/a)$. The number of collisions $\mathcal{N}_{slg}$ that occur in the wake of sling events can only be parametrized and the parametrization compared to explicit DNS results.

Here, we simply estimate $\mathcal{N}_{slg}$ as the mean flux of particles during a time of the order of the particle relaxation time τ_P,

$$\mathcal{N}_{slg} \approx 4\pi a^2 n(t_{bu} - \tau_P)|w_r^{slg}|\tau_P. \tag{17}$$

In the equation above, $n(t_{bu}-\tau_P)$ corresponds to the density taken at a time τ_P shortly before the blowup of the velocity gradient $\boldsymbol{\sigma}$. This is only an estimate of the density during the entire collision process. Another difficulty in this approach (see also [8]) is to provide a realistic estimate of the velocity difference $|w_r^{slg}|$. We will demonstrate how to properly identify the collisions induced by the sling events and how to estimate $\langle|w_r^{slg}|\rangle$ later (see Sec. IV). The sling contribution to the collision rate is then simply obtained by

$$K_{slg} = \tfrac{1}{2} n_0 f_{bu} \mathcal{N}_{slg}, \tag{18}$$

where f_{bu} is the blowup frequency defined as the average number of blowups occurring along a trajectory per unit time.

B. Numerical implementation

Our ILM requires the integration of several quantities along the trajectories of the particles such as $\mathbf{v}(t)$, $\boldsymbol{\sigma}(t)$, $n(t)$, and $\mathbf{W}(\mathbf{t})$. Integration of Eqs. (11)–(13) does not require any interpolation technique since the velocity and the velocity gradient of the fluid are given analytically by KS. The evolution equations are solved by a Runge-Kutta numerical scheme of order 2. We checked explicitly in a few cases that the results do not change when using higher-order schemes.

As already mentioned, the gradient tensor $\boldsymbol{\sigma}$ can become singular in a finite time. In order to be able to integrate the equation past the time when $\boldsymbol{\sigma}$ becomes singular, we need to regularize the problem close to the divergence. Physically, $|\boldsymbol{\sigma}| \to \infty$ implies that particles may become arbitrarily close in a finite time, which is not possible, due to the finite size of the particles. Thus, $|\boldsymbol{\sigma}|$ cannot grow by more than a factor $\sim \eta/a$. Numerically, we regularize $\boldsymbol{\sigma}$ by flipping the sign of all its component when $|\boldsymbol{\sigma}| > \tau_p^{-1}\eta/a$ [8].

Gravity is introduced via the dimensionless parameter $\epsilon_0 = \mathrm{St}\,\mathrm{Fr}$. This quantity measures the relative importance between the acceleration u_K/τ_K and the acceleration of gravity; it does not depend on the particle size. Our results are presented for two values of this parameter, $\epsilon_0 = 5.0$ and 1.0, which correspond, respectively, to weak and strong gravity.

C. Limitations about the method

While checking the ILM, we have identified two main artifacts, leading to systematic errors in the determination of the collision rates. The first problem is related to the arbitrariness in the choice of the initial velocity gradient when solving Eq. (13). Too strong a gravity, in the presence of periodic boundary conditions, also leads to incorrect estimates, as we now explain.

The ILM requires not only the position and velocity of the particles at initial time, but also of the velocity derivative $\boldsymbol{\sigma}$, needed to determine the evolution of $\mathbf{W}$. The particle positions are initialized randomly distributed, and the velocity of the particles are chosen at $t=0$ to be equal to the fluid velocity: $\mathbf{v}(t=0)=\mathbf{u}(\mathbf{x},t=0)$. As an initial for $\boldsymbol{\sigma}(0)$, we chose in most calculations $\boldsymbol{\sigma}(0)=\mathbf{h}(\mathbf{x},t=0)$. To estimate the influence of this choice, we compared with the results obtained by choosing $\boldsymbol{\sigma}(0)=0$. Not surprisingly, we found that the difference between the values of $\boldsymbol{\sigma}(t)$ corresponding to the two different initial conditions decays exponentially, with a characteristic time of the order of τ_P. In practice, after a time of order $6\tau_P$, the two solutions are indistinguishable. This implies that provided the time T needed to generate scales $\sim a$ from scales $\sim \eta$ is much larger than the characteristic time scale t_σ defined by $t_\sigma = 6\tau_P$, the estimate given by Eq. (14) does not depend on the transient regime. On the other hand, when T becomes comparable to, or smaller than t_σ, the integral in Eq. (14) becomes dominated by transient effects, so the results strongly depend on the choice of $\boldsymbol{\sigma}(0)$.

The values of the mean value of the time T needed to generate a compression of (η/a) divided by t_σ is shown in Fig. 1. Remarkably, the ratio T/t_σ seems to be essentially independent of the persistence parameter λ. The ratio T/t_σ is a decreasing function of St; it is equal to 1 for $\mathrm{St} \approx 2$. Based on the results of Fig. 1, we consider that the transient effects cannot be neglected for Stokes numbers larger than $\mathrm{St} \approx 1$. This provides a strict bound on the domain of validity of the ILM proposed in [8].

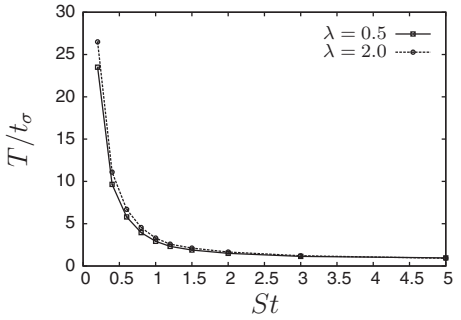

FIG. 1. Ratio between the time needed to contract a line element by a factor η/a, T, and the typical time correlation of $\boldsymbol{\sigma}$, $t_\sigma \approx 6\tau_P$. At Stokes numbers larger than ≈ 1, the time T becomes comparable to t_σ, pointing to a failure of the ILM. The gravity here is weak ($\epsilon_0 = 5$).

In a periodic domain, the effect of gravity is to introduce a drift in the direction of gravity with velocity $\mathbf{g} \times \tau_P$. With a box size of 2π, it takes a time of order $t_g = 2\pi/g\tau_P$ for a particle to settle through the entire size of the system and to be reinjected in the box. Our simulations make sense only if the time t_g is large compared the decorrelation time of the velocity field $\mathbf{u}$, $t_u \sim 1/\omega_1$, where ω_1 is the pulsation corresponding to the largest mode. At a given value of ϵ_0, this constraint sets an upper value for St. For $\mathrm{St} \leq 3$, all the results shown here are such that $t_g/t_u > 1$.

IV. DIRECT MEASUREMENTS

A. Numerical considerations

We considered the simplest case of independent monosize particles allowed to pass through each other during collisions, also known as ghost particles. We used a neighborhood search algorithm to detect the colliding particles, as introduced in [3]. Simulations have been performed over a range of Stokes numbers between 0.1 and 3 and for two different intensities of the gravity, $\epsilon_0 = 5.0$ (weak) and $\epsilon_0 = 1.0$ (strong). The particle volume fraction, $\Phi = n_0(\pi/6)a^3$, has been maintained constant and very small, $\Phi \simeq 1.2 \times 10^{-4}$, which implies that collisions involving three particles or more can be neglected. This situation is certainly appropriate in the cloud context.

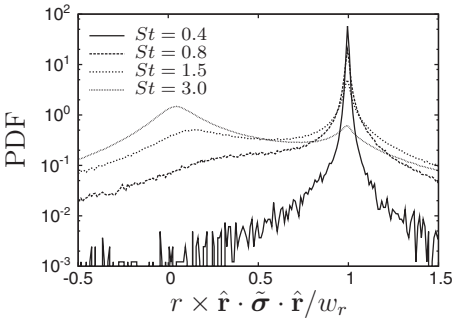

FIG. 2. PDF of the ratio between the radial relative velocity estimated by $r \times \hat{r} \cdot \tilde{\boldsymbol{\sigma}} \cdot \hat{r}$ and the real one w_r, measured at the time step preceding the contact. The parameters are $\lambda = 0.5$ and $\epsilon_0 = 5.0$.

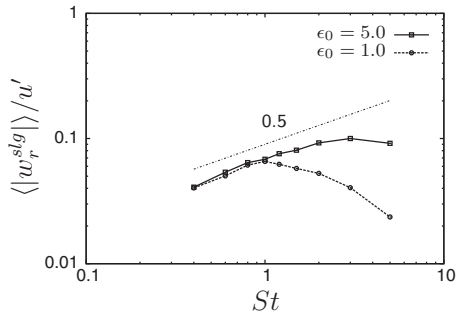

FIG. 3. Mean radial relative velocity conditioned on the sling events. This quantity behaves as $\mathrm{St}^{1/2}$ and is independent of gravity at small values of St. The persistence parameter used here is $\lambda = 0.5$.

Technically, the equations of motion have been integrated over a time long enough to observe a large number ($\sim 10^5$) of collisions. We impose a fixed volume fraction, and since the Stokes number is proportional to the square of the particles radius, the number of particles depends on the Stokes number. We took here $N_p = 10^5\ \mathrm{St}^{-3/2}$. As a result, the time of integration necessary to obtain a given number of collisions depends on St (in $\mathrm{St}^{3/2}$ for the Saffman-Turner case). Several runs were carried out with the same parameters, but with different sets of Fourier modes, so as to improve the statistics and to get an estimate of our error bars. All the measurements of the collision rate presented in this paper have been averaged over four numerical experiments.

The collision rates measured in this study are generally referred to as "geometric" because no explicit mention is made of the collision efficiency. In addition to the equations of motion (11) and (12) we also follow the evolution of the velocity gradient of each particle by integrating Eq. (13). As explained below, this allows us to identify the sling events.

B. Separating the continuous and the sling components

For a continuous collision, the radial relative velocity at contact between the two particles should be given by $w_r = a \times \hat{r} \cdot \boldsymbol{\sigma} \cdot \hat{r}$. In order to distinguish the continuous component from the sling one, we compare for each collision the real velocity difference and the quantity $r \times \hat{r} \cdot \tilde{\boldsymbol{\sigma}} \cdot \hat{r}$, computed at the time step right before the collision. In the above expression, $\tilde{\boldsymbol{\sigma}} = (\boldsymbol{\sigma}_1 + \boldsymbol{\sigma}_2)/2$, where $\boldsymbol{\sigma}_1$ and $\boldsymbol{\sigma}_2$ are the values of $\boldsymbol{\sigma}$ measured at the positions of particles 1 and 2. The probability distribution function (PDF) of the ratio of these two quantities is shown in Fig. 2. One can see clearly in this figure a quite narrow peak at $r \times \hat{r} \cdot \tilde{\boldsymbol{\sigma}} \cdot \hat{r}/w_r = 1$. This peak corresponds to the continuous contribution to the collision rate. In this case, the radial relative velocity can be evaluated from the gradient velocity tensor. As the Stokes number decreases, the peak around 1 becomes weaker, and a much broader peak develops around $r \times \hat{r} \cdot \tilde{\boldsymbol{\sigma}} \cdot \hat{r}/w_r = 0$ (see Fig. 2). The latter peak corresponds to velocity differences between colliding particles much larger than the value expected based on the velocity gradient $\tilde{\boldsymbol{\sigma}}$ and is thus attributed to the sling collisions. In order to evaluate the two separate contributions to the collision rate, we simply distinguish the nature of the

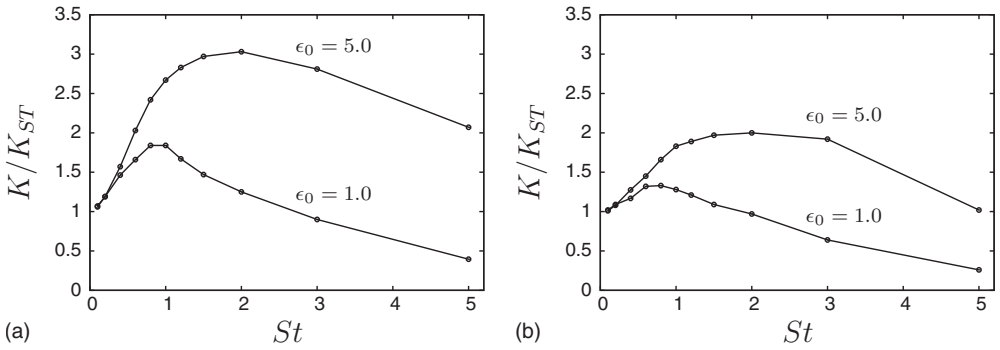

FIG. 4. Direct measurements of the total collision rate K normalized by the Saffman-Turner collision rate K_{ST} for two different values of the time correlation of the fluid: (a) $\lambda=0.5$ and (b) $\lambda=2.0$. Increasing gravity or decreasing the time correlations tends to decrease the collision rate.

collision according to the value of the ratio $r\times\hat{r}\cdot\tilde{\boldsymbol{\sigma}}\cdot\hat{r}/w_r$. We thus use the following simple criterion: collisions satisfying the criterion $1-\delta/2<r\times\hat{r}\cdot\tilde{\boldsymbol{\sigma}}\cdot\hat{r}/w_r<1+\delta/2$ are considered as contributing to the regular term, and otherwise to the sling term. The choice of δ is somewhat arbitrary. It should be large enough, so at small value of the Stokes number, where $f_{bu}\approx 0$, the sling contribution is effectively zero. We chose $\delta=0.15$ and partially took into account the uncertainty introduced by this choice by increasing the error bars by a factor of 50% in Figs. 5–8 shown below.

This method thus allows us also to identify the velocity statistics of the radial velocity between colliding particles $|w_r^{slg}|$ during a sling event. Of particular interest to the ILM is the mean value $\langle|w_r^{slg}|\rangle$, which was found to be well approximated by a form $\langle|w_r^{slg}|\rangle\approx A\ \mathrm{St}^{1/2}$ (see Fig. 3). This functional form, obtained numerically at moderate values of the Stokes number ($\mathrm{St}\lesssim 1$), differs from the functional form derived in [7] in the very large Stokes number limit. In this case one rather finds a dependence like $\langle|w_r^{slg}|\rangle\approx A'\ \mathrm{St}^{-1/2}$.

The qualitative behavior of the dependence of the velocity $\langle|w_r^{slg}|\rangle$ differs from the very phenomenological description proposed in [8], which was effectively assuming that the velocity difference $\langle|w_r^{slg}|\rangle$ was proportional to $\sim\eta/\tau_K\times\mathrm{St}^{-1/2}$, instead of $\mathrm{St}^{1/2}$. Interestingly, the results of [18,19] suggest $\Delta v\sim\tau_P^{1/2}$ when $\tau_K\ll\tau_P$, under the condition that τ_P is smaller than the correlation time at the largest scale, which effectively implies a $\langle|w_r^{slg}|\rangle\sim\eta/\tau_K\times\mathrm{St}^{+1/2}$ dependence. The results of [18,19] thus provide a natural explanation of our own observation.

V. NUMERICAL DETERMINATION OF THE COLLISION RATES

The results of our direct measurements of the total collision rate are shown in Fig. 4. At very low gravity ($\epsilon_0=5.0$) the curves exhibit a behavior qualitatively very similar to the one observed in the DNS of [3] in the absence of gravity. A very strong growth of the collision rate is observed at small values of the Stokes number, followed by a slow decrease after reaching a maximum at about $\mathrm{St}\simeq 2$. Figure 4 reveals that small time correlations (large values of λ) as well as strong gravity (small values of ϵ_0) tend to decrease the collision frequency. This is consistent with the observation that both effects independently reduce preferential concentration. Indeed, gravity decreases clustering since it reduces the interaction time between particles and the turbulent eddies [20,21]. The effect of λ has been considered in [22]. It was shown that, in two-dimensional KS flows, particles and velocity stagnation points of the flow anticluster. The persistence of the stagnation points diminishes when the value of λ increases, thus inhibiting the formation of clusters, therefore diminishing the preferential concentration effect.

The comparison between the results obtained with the ILM and the measurements for the continuous component of the collision rate, obtained by directly counting the number of collisions, is shown in Fig. 5. As expected from Fig. 1 and from the resulting discussion, the ILM does not permit us to evaluate the collision frequency for large Stokes; for this reason we only show the results for $\mathrm{St}\leq 0.8$. From the direct

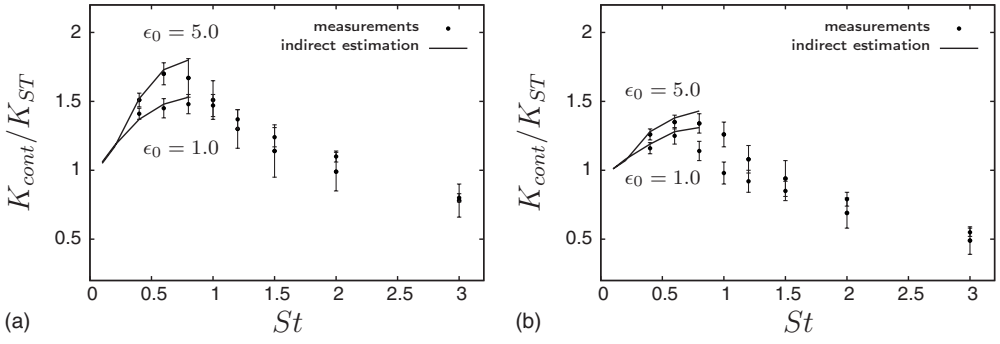

FIG. 5. Comparison between direct measurements and the calculations based on the ILM of the continuous contribution for two different values of the time correlation of the fluid: (a) $\lambda=0.5$ and (b) $\lambda=2.0$. The results obtained by the indirect Lagrangian method are not shown for $\mathrm{St}>0.8$ because of the inconsistency of the method for large St.

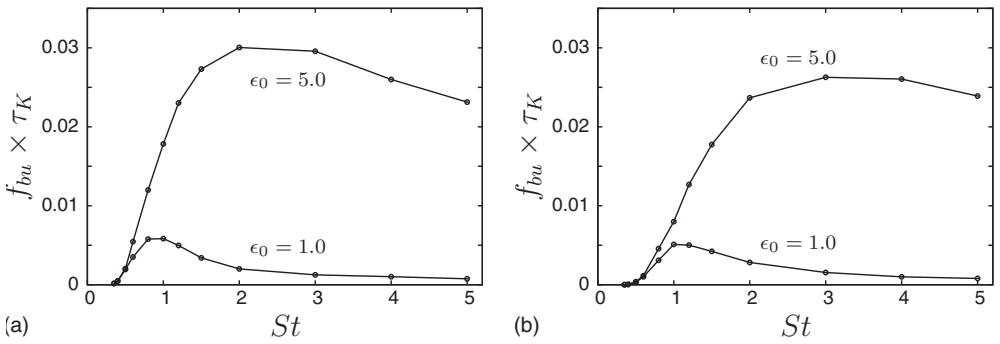

FIG. 6. Average blowup frequency f_{bu} normalized by the Kolmogorov time τ_K for two different values of the time correlation of the fluid: (a) $\lambda=0.5$ and (b) $\lambda=2.0$. Gravity reduces dramatically the probability for a particle to experience a sling event.

measurements we see that the continuous part of the collision rate reaches a maximum around $\mathrm{St}\sim 0.6-0.8$, then decreases and finally becomes smaller than the ST case. Looking at Eq. (14), one can see that the growth of K_{cont} can only be attributed to preferential concentration. Those results reflect that the preferential concentration is largest for $\mathrm{St}\sim 0.6-0.8$.

The effect of gravity is to reduce the intensity of this phenomenon, so the values of K_{cont} are smaller for $\epsilon_0=1$ than for $\epsilon_0=5$. For the continuous component, a smaller value of the correlation time (increased value of λ) also leads to a reduction in the collision rate. This is also consistent with the observation (see [22]) that preferential concentration is reduced at larger values of λ.

Figure 6 shows the behavior of the blowup frequency with respect to the Stokes number, a crucial quantity for the determination of the sling component [Eq. (18)]. We found, as in [8] that $f_{bu}\tau_K$ could be well represented by an analytical expression of the form $f_{bu}\tau_K=\exp(-A/\mathrm{St})\mathrm{St}^{-2}(B+C\,\mathrm{St}^D)$. The asymptotic behavior $\exp(-A/\mathrm{St})$ for Stokes going to zero can be theoretically justified (see [23,24]). In more elementary terms, it is a manifestation of the intrinsic lack of analyticity of the problem since flipping the sign of the Stokes number leads to a physically ill-defined problem [25].

Figure 6 implies that increasing the gravity significantly reduces the blowup frequency. In fact, when the terminal velocity ($\mathbf{v}_T\equiv\mathbf{g}\times\tau_P$) becomes too large, particles fall through the flow eddies and cannot be accelerated enough to be shot out by the vortices.

In the range of parameters considered here, the effect of the parameter λ, which describes the persistence of the flow, affects essentially the parameter A: $A\simeq 3.1$ for $\lambda=0.5$ and $A\simeq 4.0$ for $\lambda=2$. Thus, at higher values of λ, the blowup frequency is very much reduced. This is consistent with the naive intuition based on Eq. (13) that a blowup of $\boldsymbol{\sigma}$ requires a large value of the fluid velocity gradient h for a long enough time. Increasing λ is bound to decrease the probability of such an event. In practice, for $\mathrm{St}<0.2-0.3$ the blowup frequency is essentially zero.

The comparison between the results obtained with the ILM, assuming a velocity difference behaving like $\langle|w_r^{slg}|\rangle \sim \eta/\tau_K\times\mathrm{St}^{1/2}$, and the measurements of the sling contribution to the collision rate is shown in Fig. 7. As it was the case for the continuous contribution (see Fig. 5), the ILM does not allow us to predict correctly the collision rate for values higher than $\mathrm{St}\gtrsim 1$. The agreement between the two estimates is somewhat better than what was found for the continuous contribution. The direct measurements show a maximum of the sling contribution in the range $1\leq\mathrm{St}\leq 2$. With the value for the velocity difference, the ILM does not capture this maximum.

We note that the functional form proposed in [8] on phenomenological grounds, $\langle|w_r^{slg}|\rangle\sim\eta/\tau_K\times\mathrm{St}^{-1/2}$, captures much better the qualitative aspect of the sling contribution to the collision curves, up to much larger values of the Stokes number (see Fig. 8). The quality of the fit at values in the range $0.4\lesssim\mathrm{St}\lesssim 1$ is not too sensitive to the power law used; the difference is much more visible for $\mathrm{St}\gtrsim 1$.

A qualitative justification may be provided by the theoretical results of [7] suggesting a $\langle|w_r^{slg}|\rangle\sim\mathrm{St}^{-1/2}$ behavior at large values of St for a flow with a single scale. We note that

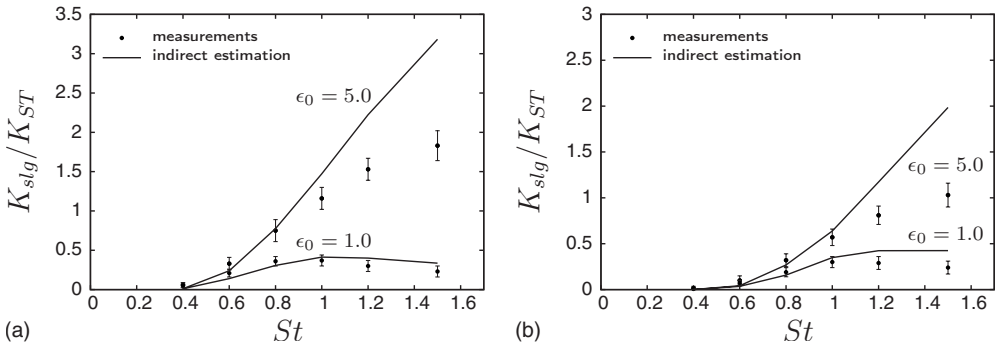

FIG. 7. Comparison between direct measurements and the calculations based on the ILM of the sling contribution for two different values of the time correlation of the fluid: (a) $\lambda=0.5$ and (b) $\lambda=2.0$. The results obtained by direct counting of the collision rates are correctly captured by the ILM only up to $\mathrm{St}\gtrsim 1$.

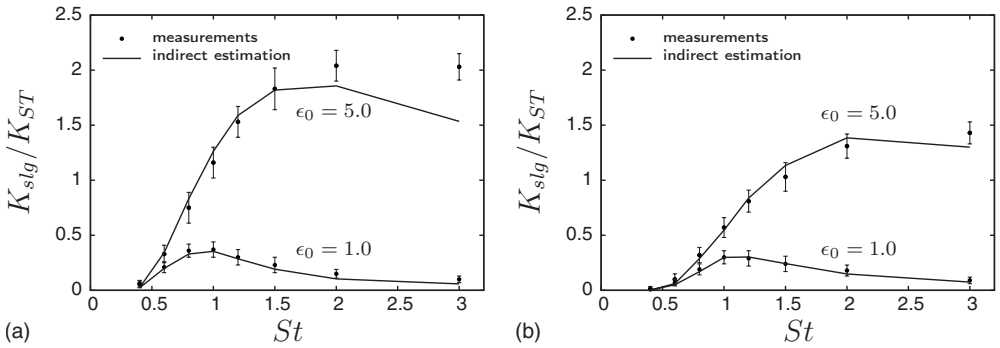

FIG. 8. Modified description of the sling term. The sling contribution to the collision rate is much better captured by the form originally proposed in [7,8], with a collision velocity between particles behaving like $w_r^{slg} \sim A' \, \mathrm{St}^{-1/2}$ and justified in the limit of very large Stokes numbers. The calculations have been carried out with two different values of λ: (a) λ=0.5 and (b) λ=2.

the prediction of [18,19] suggesting a $\mathrm{St}^{1/2}$ behavior for a multiscale flow applies only when τ_P satisfies $\tau_K \ll \tau_P < L/U$, where L/U is the eddy turnover time (i.e., the correlation of the velocity at large scale); hence, it does not apply at too large value of τ_P, consistent with the observation that the $\langle |w_r^{slg}| \rangle \sim \eta/\tau_K \times \mathrm{St}^{1/2}$ behavior is valid only up to a finite value of the Stokes number (see Fig. 3). At large values of τ_P, particles should be sensitive only to the largest eddies in the flow, thus suggesting an explanation as to why the fit shown in Fig. 8 is much better at $\mathrm{St} \gtrsim 1$ than the one shown in Fig. 7. We notice however that Fig. 3 does not clearly support the $\langle |w_r^{slg}| \rangle \sim \eta/\tau_K \times \mathrm{St}^{-1/2}$ behavior at very large values of St. This points to a weakness of our analysis and suggests that further work is necessary to understand the good agreement between the fit shown in Fig. 8 and the numerical results.

VI. SUMMARY AND DISCUSSIONS

In this work, we have studied collisions occurring in a monodisperse very dilute suspension of heavy particles in a synthetic turbulent flow. The collision rates were estimated both by directly counting how often two particle centers get closer than a particle diameter a (direct method) and the results have been compared systematically with the ILM, proposed recently in [8].

One of the main objectives of the work was to investigate the possibility to separate the contributions to the collision term induced by the gradients of the turbulent flow (the "regular contribution") from the contribution induced during sling events or caustics formation. By systematically monitoring the velocity difference between the particles during a collision, and by comparing it with the time local gradient of the particle flow, we have been able to clearly separate the contribution due to the two effects. For modeling purposes, we find that the mean velocity difference induced during the sling events goes as $\langle |w_r^{slg}| \rangle \sim \mathrm{St}^{1/2}$. This result is at odd with the phenomenological considerations in [8], which rather postulated a dependence of the form $\langle |w_r^{slg}| \rangle \sim \mathrm{St}^{-1/2}$.

The other objective was to compare the collision rates determined by direct counting and by the ILM proposed in [8]. The main result of this work is that the ILM provides quantitatively very accurate results for a wide range of Stokes numbers, as well as for a wide range of gravity strength, as measured by the parameter ϵ_0. In the absence of gravity, the ILM works only at limited Stokes numbers ($\mathrm{St} \lesssim 1-2$). Incorporating the effect of gravity provides additional constraints when the free fall velocity of the droplets becomes too fast.

These results validate further the good qualitative agreement found in Navier-Stokes flows between direct estimates of collision rates at limited Reynolds numbers $R_\lambda \approx 50$, in a limited range of Stokes numbers ($0.1 \leq \mathrm{St} \leq 0.4$ [9,20]) for the regular contribution of the collision rate, prevalent at small Stokes numbers. It also sheds light on the systematic difference between the sling contributions that can easily be attributed to the incorrect parametrization of $\langle |w_r^{slg}| \rangle$. One of the consequences of our work is that the calculations based on the ILM cannot be trusted for Stokes numbers larger than $\mathrm{St} \gtrsim 1$.

Clearly identifying the physical mechanisms leading to an enhancement of the collision rates between inertial particles in turbulent flows is very significant, in view of the many physical situations where collisions play a crucial role. The sling effect, recently identified as one of the key mechanisms in determining the collision rate between inertial particles [6,7] is difficult to model from first principles. Our results allow us to extract from a numerical study the important features necessary to estimate the collision rate due to sling events. With this ingredient, the ILM-based estimate of the collision rate proposed in [8] leads to a quantitatively accurate description of the collision rate in the range $0 \leq \mathrm{St} \lesssim 1$. Although still incomplete, the understanding gained in this work should help in providing a reliable parametrization of the collision rate in the parameter range relevant to engineering or natural flow situations.

ACKNOWLEDGMENT

This work was supported by the Agence National pour la Recherche (Contract DSPET) and by IDRIS.

[1] P. G. Saffman and J. S. Turner, J. Fluid Mech. **1**, 16 (1956).
[2] H. R. Pruppacher and J. D. Klett, *Microphysics of Clouds and Precipitation* (Kluwer, Dordrecht, 1997).
[3] S. Sundaram and L. R. Collins, J. Fluid Mech. **335**, 75 (1997).
[4] L. P. Wang, A. S. Wexler, and Y. Zhou, Phys. Fluids **10**, 2647 (1998).
[5] J. Abrahamson, Chem. Eng. Sci. **30**, 1371 (1975).
[6] G. Falkovich, A. Fouxon, and M. G. Stepanov, Nature (London) **419**, 151 (2002).
[7] M. Wilkinson, B. Mehlig, and V. Bezuglyy, Phys. Rev. Lett. **97**, 048501 (2006).
[8] G. Falkovich and A. Pumir, J. Atmos. Sci. **64**, 4497 (2007).
[9] C. N. Franklin, P. A. Vaillancourt, M. K. Yau, and P. Bartello, J. Atmos. Sci. **62**, 2451 (2005).
[10] B. Andersson, K. Gustavsson, B. Mehlig, and M. Wilkinson, EPL **80**, 69001 (2007).
[11] K. Gustavsson, B. Mehlig, and M. Wilkinson, New J. Phys. **10**, 075014 (2008).
[12] J. C. H. Fung *et al.*, J. Fluid Mech. **236**, 281 (1992).
[13] J. C. H. Fung and J. C. Vassilicos, Phys. Rev. E **57**, 1677 (1998).
[14] M. A. I. Khan and J. C. Vassilicos, Phys. Fluids **16**, 216 (2004).
[15] F. Nicolleau, K.-S. Sung and J. C. VassilicosPhys. Rev. E **78**, 046306 (2008).
[16] L. Ducasse and A. Pumir, Phys. Rev. E **77**, 066304 (2008).
[17] M. R. Maxey and J. J. Riley, Phys. Fluids **26**, 883 (1983).
[18] B. Mehlig, V. Uski, and M. Wilkinson, Phys. Fluids **19**, 098107 (2007).
[19] K. Gustavsson, B. Mehlig, M. Wilkinson, and V. Uski, Phys. Rev. Lett. **101**, 174503 (2008).
[20] L. P. Wang, A. Orlando, S. E. Kasprzak, and W. W. Grabowski, J. Atmos. Sci. **62**, 2433 (2005).
[21] P. Vaillancourt, M. Yau, P. Bartello, and W. W. Grabowski, J. Atmos. Sci. **59**, 3421 (2002).
[22] L. Chen, S. Goto, and J. C. Vassilicos, J. Fluid Mech. **553**, 143 (2006).
[23] M. Wilkinson and B. Mehlig, EPL **71**, 186 (2005).
[24] S. Derevyanko, G. Falkovich, K. Turitsyn, and S. Turitsyn, J. Turbul. **8**, 16 (2007).
[25] F. J. Dyson, Phys. Rev. **85**, 631 (1952).